JETIR.ORG ISSN: 2349-5162 | ESTD Year : 2014 | Monthly Issue
JOURNAL OF EMERGING TECHNOLOGIES AND INNOVATIVE RESEARCH (JETIR)
An International Scholarly Open Access, Peer-reviewed, Refereed Journal

Investigation of the variation of temperature and refractive index on the output performance of a core length of a multi-mode optic fiber

[1] Aideyan. Osaro.D and [2] Samson. Linus. M
[1,2]Department of Mathematics and Statistics, Taraba State University Jalingo, Nigeria.
Corresponding Author's; email: osaro.aideyan@tsuniversity.edu.ng

Abstract

This study investigates how temperature and surrounding refractive index affect the output performance of a multimode optical fiber. A multimode fiber core segment was immersed in aqueous sugar solutions of varied concentration (0–40 g/100 mL) while temperature was varied from room temperature up to elevated values. Solution refractive indices were measured and correlated with concentration; their temperature dependence was quantified. Fiber output power and near-field intensity distribution were recorded as functions of ambient refractive index and temperature. Results show minimal change in refractive index for concentrations below 2.5 g/100 mL, a nearly constant (dormant) region up to ≈5 g/100 mL, and a linear increase in refractive index above that point with correlation constant $\gamma = 1.5\times10-3$ (g/100 mL) $^{-1}$. Temperature coefficients of refractive index for 20 g/100 mL and 40 g/100 mL solutions were $-1.53\times10-4$ °C−1 and $-2.1\times10-4$ °C−1, respectively. Corresponding fiber output power decreased measurably when the external refractive index approached the core index and with rising temperature; mode distribution broadened under conditions of reduced index contrast. These findings clarify how environmental refractive index and temperature degrade multimode fiber output and support applications in optical sensing and communications.

Key Words: Optical fiber; Concentration; Refractive index; Sugar solution and Temperature

1.0 Introduction and Background

Optical fibers underpin modern communications, sensing, and photonic systems (Xin.,2026 and Butt et al., 2024). Multimode optical fibers (MMFs) are widely used where high coupling efficiency, relaxed alignment tolerances, and cost-effectiveness matter (Li et al., 2024 and Liu et al., 2022). However, output performance of an MMF including modal power distribution, speckle patterns, insertion loss, beam quality, and effective numerical aperture depends sensitively on environmental and physical parameters (Wang., 2023, Tuomola., 2023 and Chapalo et al., 2024). Two key variables are temperature and refractive index (RI) of the fiber core and its surroundings. Understanding how these variables interact with core length to influence output performance is essential for improving fiber-based sensors, high-power delivery systems, and reliable data links in variable environments.

Temperature affects MMF behavior both directly, via thermo-optic and thermal expansion effects in the core and cladding materials, and indirectly, by altering stress and birefringence (Du.,2025, Meehan., 2024 and Yang et al., 2025). The thermo-optic coefficient (dn/dT) typically causes refractive index changes with temperature, shifting modal effective indices and altering phase relationships among guided modes (Yang., 2025, Butt., 2025 and Jiao., 2025). Thermal expansion modifies geometric parameters (core radius, numerical aperture), further changing modal cutoff and coupling conditions. (Tan., 2023 and Zhao., 2023) These combined effects can cause temperature-dependent modal redistribution, speckle decorrelation, and wavelength-dependent transmission changes. (Minds and Light., 2016).

Prior experimental studies have shown measurable shifts in modal power distribution and speckle contrast with temperature variations on centimeter to meter fiber lengths, with magnitude depending on core glass composition, dopants, and coating. (Efendioglu.,2025 and Ramachandran., 2025).

Refractive index variations whether intrinsic (material inhomogeneity, dopant concentration) or extrinsic (surrounding medium RI, applied coatings, or index-matching fluids) directly change the waveguide condition. (Danko., 2020 and Camici., 2021). Small RI changes at the core or cladding boundary modify confinement, mode-field diameters, and effective indices, which influence modal interference at the output (Shere.,2023 and Chen et al., 2025). For sensing applications, deliberate variation of surrounding RI has been exploited to create refractometric sensors based on modal loss or speckle analysis (Sun et al 2023 and Nedoma et al., 2026). Studies

of MMF length dependence indicate that longer cores promote increased mode mixing and modal dispersion, often leading to more stable time-averaged output but potentially reduced sensitivity to localized perturbations (Kant et al., 2024 and Guo et al., 2026)

Core length itself is a controlling parameter, short sections may preserve input modal content more, making output highly sensitive to local RI or temperature changes; long cores tend to average modal phases via mode coupling, reducing sensitivity to small perturbations but increasing modal noise and dispersion effects. The interplay among temperature, refractive index changes, and core length defines a parameter space where output metrics (e.g., transmitted power, modal noise, beam quality M2, speckle correlation) vary nonlinearly.

Despite previous work on individual effects, comprehensive studies that map combined temperature and RI variations across a controlled range of core lengths are limited. Gaps include quantitative models linking dn/dT and thermo-mechanical changes to modal coupling statistics in MMFs and systematic experimental datasets across lengths from millimeters to meters. This research addresses the insufficient understanding of how simultaneous variations in temperature and refractive index affect the output performance of multimode optical fibers as a function of core length. The goal of this work is to produce quantitative characterization and modeling that enable robust design and calibration of MMF systems and sensors operating under simultaneous temperature and refractive-index fluctuations.

2.0 Theory of Intensity Modulated Sensors

Amplitude-modulated optical fiber sensors represent a foundational paradigm in fiber optic sensing due to their operational and architectural simplicity, which has led to their extensive investigation within the field (Kumar, 2006). The transduction mechanism in these sensors is based on the modulation of the optical power, or intensity, propagating within the fiber core's sensing region. When an external perturbation, denoted by the generalized coordinate is applied, it induces a variation in the transmitted optical amplitude. Consequently, the electric field propagating through the fiber, {E}(z, t), can be expressed as a carrier wave whose amplitude is a function of the perturbation. A generalized representation of this field is given by

$$E(z,t) = E_0 \cos\theta \quad (1)$$

where $\theta = \beta L$ and $\beta = 2\pi/K$

K is the propagation constant and L is the length of the fiber. The intensity, I is given as

$$I = |E|^2 = E_0^2 Cos^2\theta \quad (2)$$

In the presence of perturbation, P, then θ can further be expressed as:

$$\frac{d\theta}{dP} = L\frac{d\beta}{dP} + \beta\frac{dL}{dP} \quad (3)$$

The expression in Equation (3) formalizes the opto-mechanical coupling within the fiber. Specifically, the term on the left-hand side characterizes the mechanical deformation of the fiber structure, while the term on the right-hand side represents the resulting variation in the refractive index, Δn. The modulation of the optical intensity, ΔI, induced by the external perturbation parameter P, is given by

$$\frac{dI}{dP} = \frac{dI}{d\theta} \times \frac{d\theta}{dP} = 2E_0^2 Cos\beta L Sin\beta L \frac{d\theta}{dP}$$

$$= E_0^2 (Sin2\beta L)(L\frac{d\beta}{dP} + \beta\frac{dL}{dP}) \quad (4)$$

It is evident from Equation (4) that the variation in optical intensity, denoted (ΔI), induced by an external perturbation (P), is directly proportional to the resultant geometric deformation of the fiber structure and the concomitant modification of its refractive index profile.

A principal advantage of this intensity-modulated sensing modality lies in its direct measurement of the optical power at the fiber terminus. This parameter constitutes the fundamental observable in virtually all fiber-optic sensing architectures and can be resolved with a high degree of precision. The system's operational constraints, specifically the received optical power and the required detection bandwidth, dictate that the fundamental limit to intensity sensitivity is governed by two primary stochastic noise processes: shot noise, arising from the discrete and statistical nature of photon arrival events at the detector, and thermal (Johnson-Nyquist) noise within the detection circuitry.

Under these conditions, the signal-to-noise ratio (SNR), with specific emphasis on the thermal noise contribution, is given by the following expression (Kumar, 2006):

$$SNR = \frac{\eta_{eff} P_*}{h\nu W_\lambda} \quad (5)$$

where P_* is the optical power incident on the detector, η_{eff} is the quantum efficiency of the detector, $h\nu$ is the photon energy, W_λ is the bandwidth of the optical receiver.

3.0 Research Methodology

The experimental set-up of the optical fiber sensor is shown in Fig 1. For a clean optical fiber core, the outer jacket was first removed and gently washed in distilled water. This was then allowed to dry for some time and the desired length to be un-cladded on the optical fiber was carefully removed and then dipped in dichloromethane (methyl chloride) solution so that the cladding material was completely removed. Solutions of different concentrations were prepared by weighing out specific grams of analar sugar using an electronic top loading balance, Model: Scoutpro SP 202, (0 - 200g max). The solute was allowed to dissolve in distilled water in a 100 ml measuring cylinder before making up to mark. The refractive indices of these solutions were determined using Abbe-Refractometer, (Model: 2WAJ). The optical source and the detector were then connected and power was launched into the 1.0 m length of the optical fiber patch cord. The output power at the other end was recorded. At the center of the patch code, a 1.0 cm length was un-cladded and immersed into a trough, (a wide mouth plastic bath) containing the prepared sugar solution of known concentrations and refractive indices at room temperature. The new power output was then recorded for the same wavelength of the initial power launched. First, by keeping a fixed un-cladded length, concentration and temperature, and secondly, for a fixed concentration and temperature with varied un-cladded lengths. Finally, temperature effect on concentration was investigated. The experimental set-up for the measurement of temperature effect on refractive index is shown in Figure 1.

Fig.1 ***Experimental set up of the optical fiber sensor***

4.0 Results and Discussion

The results obtained are as presented in tables 1, 2 and 3. We observed that the variation in the refractive indices for concentrations of 1.0g/100 ml to 4.5g/100 ml and observed its effect on the MMF which is seen to appears very minimal, and this can be associated to the insignificant change in the density of the sugar solution which forms the control to ascertain the effect of refractive index on MMF

Table 1: Values of Sugar Solution Concentration and Refractive index at room Temperature, 37^0C

S/N	Sol. Con. (g/100 ml)	Refractive index, n
1	0	1.3251
2	1.0	1.3254
3	1.5	1.3257
4	2.0	1.3260
5	2.5	1.3263
6	3.0	1.3267
7	3.5	1.3278
8	4.0	1.3292
9	4.5	1.3296
10	5.0	1.3324
11	5.5	1.3343
12	6.0	1.3365
13	6.5	1.3367
14	7.0	1.3379
15	7.5	1.3393
16	8.0	1.3402
17	10	1.3436

18	15	1.3515
19	20	1.3586
20	25	1.3658
21	30	1.3721
22	35	1.3794
23	40	1.3867

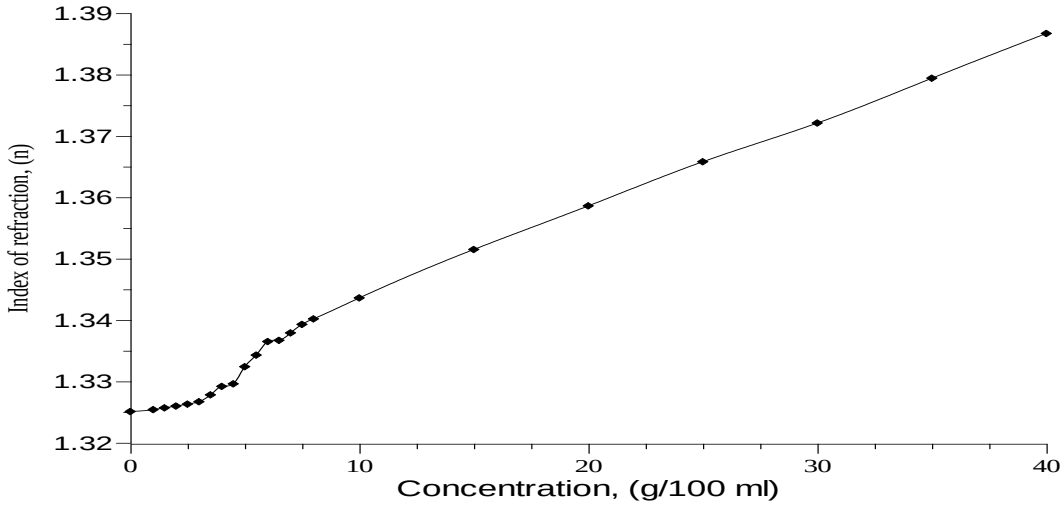

Figure 2. Graph of refractive index versus concentration of Sugar solution

The plot of refractive index of the annular sugar solution with concentration is shown in Fig 2. Refractive index is found to be fairly constant up to the solution concentration of 4.5g/100 ml, and changes above these values. The refractive index is observed to be linearly dependent on the concentration above this. On this note, we considered only solutions of concentration 5g/100 ml to 40g/100 ml. With decrease in concentration, the density of the solution also decreases resulting in the decrease in refractive index. The result shows that the refractive index of the sugar solution of concentration less than 4.5g/100 ml measures nearly the same as that of pure water at room temperature. The result indicates that the effect of concentration on refractive index is dominant up to the concentration level of about 5g/100 ml. Because of this dormancy of the concentration on refractive indices, (1g/100 ml to 4.5g/100 ml), the graph was extrapolated for 5g/100 ml and above. This shows that the refractive index of the solvent at zero concentration of the solute at room temperature, 37^0C is 1.3273

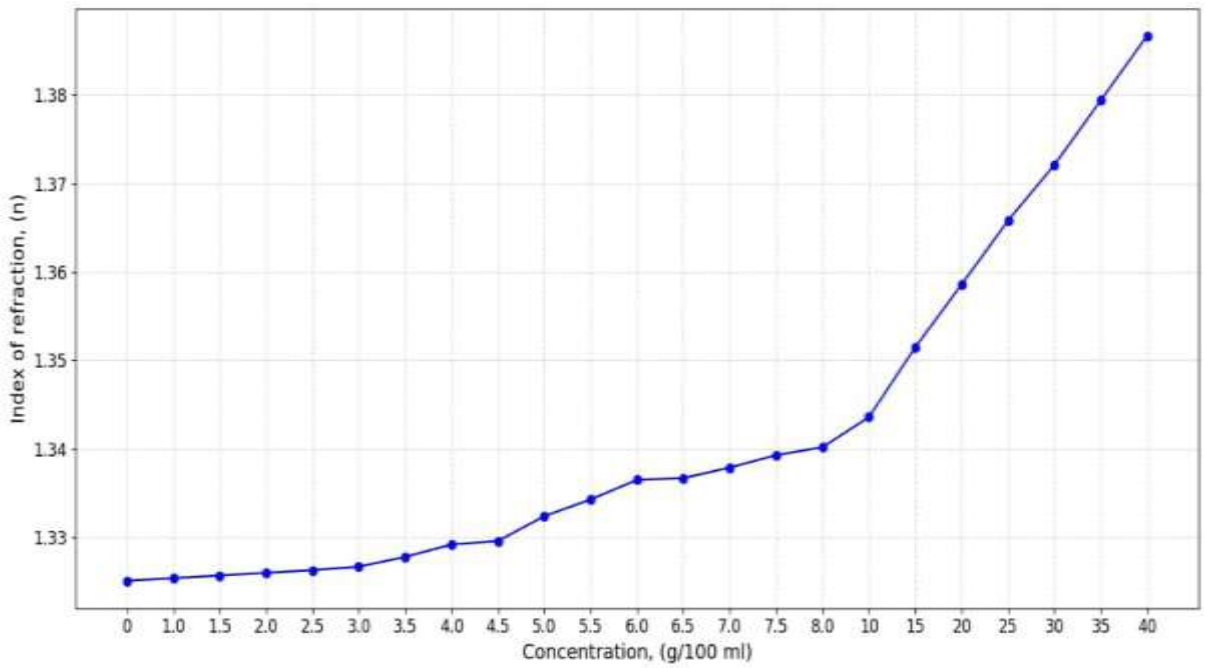

Fig. 2 ***Graph of refractive index vs Concentration (>5g/100 ml)***

(i) Effect of Temperature on Refractive index

Two of these solutions, of concentrations, 20g/100 ml and 40g/100 ml, with refractive indices 1.3586 and 1.3867 respectively were subjected to heat between temperatures of 37 to 70 ^{0}C and the corresponding values of the refractive index were determined. This was achieved with the aid of a thermostatic bath, water pump that helps in circulating the regulated temperature of the water into the refractometer's lower and upper columns (See plate I).

Table 2: Data on Temperature effect on the Refractive index of the two different Concentrations: (a) Solution Concentration of 20 g/100 ml and (b) 40 g/100 ml

(a)

S/N	Sol. Conc. 20g/100 ml	
	Temp. ^{o}C	Refractive index, n
1	37.0	1.359
2	40.0	1.358
3	45.0	1.358
4	50.0	1.357
5	55.0	1.356
6	60.0	1.355
7	65.0	1.355
8	70.0	1.353

(b)

S/N	Sol. Conc. 40g/100 ml	
	Temp. ^{o}C	Refractive index, n
1	37.0	1.387
2	40.0	1.386
3	45.0	1.385
4	50.0	1.384
5	55.0	1.383
6	60.0	1.382
7	65.0	1.381
8	70.0	1.380

A plot of refractive index as a function of temperature is shown in fig 4. The variations of refractive index for both concentrations are found to be inversely proportional to temperature. The temperature coefficient (dn/dT) for 20g/100 ml and 40g/100 ml concentrations were found to be $-1.5311\times10^{-4}/\ ^{0}C$ and $-2.1210\times10^{-4}/\ ^{0}C$ respectively.

The result shows that the refractive index is inversely proportional to temperature for the two different concentration.

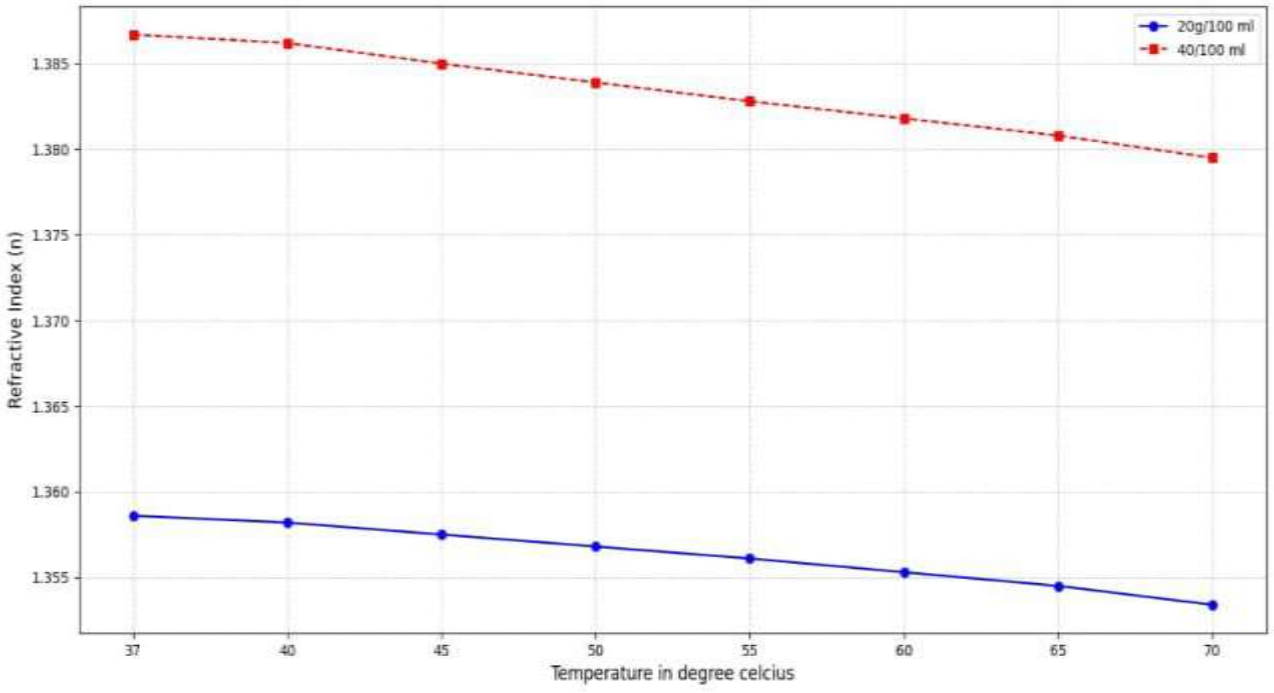

Fig 4: *Graph of refractive index vs temperature for 20g/100 ml and 40 g/100 ml Concentrations*

(ii) Power output variation on Core length of the Optical Fiber

Readings for the output power for the three different uncladded lengths of 1.0, 2.0 and 3.0 cm were taken for the sugar solution concentrations between 0 to 40g/100 ml. This result is presented in table 3. The result shows that: At the same concentration, the output power decreases with increase of the un - cladded length of the optical fiber. For each fixed length, the output power decreases with increase in the concentration of the sugar solution. Therefore, for any given solution of known concentration, the output power decreases exponentially.

Table 3: Values of Power output for the un-cladded lengths of the optical fiber patch cord immersed in the solutions at a source wavelength, $\lambda = 1300$ nm. (Power output before un-cladding, $P_0 = 48.82$ (-dBm).

	Sol.Conc.(g/100ml)	Power output (dBm)		
S/n		Uncladded length of optic fibers	Uncladded length of optic fibers	Uncladded length of optic fibers
		1.0cm	2.0cm	3.0cm
1	0	47.00	48.88	48.93
2	5	48.83	48.89	48.94
3	10	48.84	48.90	48.95
4	15	48.85	48.92	48.97
5	20	48.86	48.95	49.00
6	25	48.87	48.99	49.04
7	30	48.89	49.03	49.09
8	35	49.03	49.09	49.15
9	40	49.10	49.16	49.22

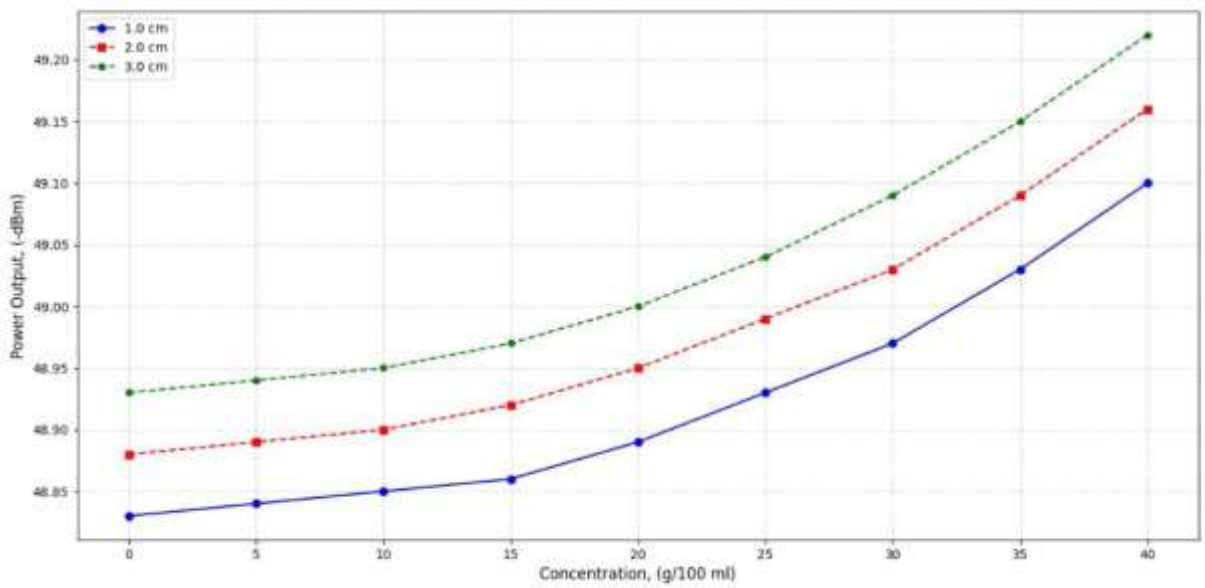

Fig 5: *Graph of Power output vs refractive index for concentration for the un-cladded Lengths of 1, 2, 3 cm of the optical fiber immersed in solution.*

In Fig 5, the decrease in the output power is as a result of the variation of the refractive index of the guiding liquid solution with respect to that of the core of the optical fiber. The decrease in output power observed as concentration increases is in agreement with Lorentz - Lorenz equation, sometimes referred to as Clausius - Mossotti equation and Maxwell's equation with the general form.

$$\frac{n^2-1}{n^2-2}\frac{1}{\rho}=\frac{N}{M} \tag{6}$$

For a transparent medium, the relation

$$\frac{n^2-1}{n^2-2}\frac{1}{\rho}=Cons\tan t \tag{7}$$

where N is the molar refractivity, M is the molar mass, ρ the density and n the refractive index. (Goldstein, 1996). That is, in a homogeneous solution, the power of light been transmitted through decreases as the refractive index increases.

5.0 Conclusion

We have experimentally investigated the coupled effects of thermal variation on the refractive index profile of a liquid medium and the subsequent influence of refractive index on the propagation characteristics of a multimode optical fiber. The analysis was conducted over a thermal range of T = [37, 70] ºC. Maintaining a fixed optical

wavelength, the empirical data indicate that the transmitted optical power is contingent upon the length of the exposed fiber core. In the reference state of zero concentration, this power is solely a function of said length. Upon introduction of the solute, the output power exhibits a strictly decreasing trend correlated with the elevation of both the solute concentration and the corresponding refractive index of the liquid medium. The refractive index remains largely invariant for concentrations below 4.5 g/100 ml due to minimal density changes, but becomes linearly dependent on concentration above this critical value. However, the refractive indices of the concentrations below 2.5 g/ml measures nearly as that of distilled water. The temperature coefficients for the refractive index of the two concentrations give nearly a constant value. The output power from the optical fiber was found to decrease exponentially which is also in agreement with the Lorentz- Lorenz equation. The dependence of the observed phenomena upon the source wavelength, which was maintained as a fixed parameter in the present work, has not been addressed here and remains a subject for subsequent analysis. The findings, however, are anticipated to be of relevance to applications in Mathematical modelling, analytical Chemistry and optical fiber communications

Authors contributions: D.O.Aideyan: Conceptualization, Methodology, SoftwareValidation, writing original draft, Writing review & editing. **S. Linus:** Supervision, writing original draft, Writing review & editing.

Acknowledgement: Authors are grateful to the Taraba State University and Tetfund IBR Grants for their financial support throughout this research. We are also grateful to National center for remote sensing Jos, Plateau State, Nigeria for their characterization supports.

Disclosure statement: *Conflict of interest:* Authors declare that there are no conflicts of interest.

Reference

Butt, M. A., Mateos, X., & Piramidowicz, R. (2024). Photonics sensors: a perspective on current advancements, emerging challenges, and potential solutions. *Physics Letters A*, *516*, 129633.

Butt, M. A. (2025). Emerging Trends in Thermo-Optic and Electro-Optic Materials for Tunable Photonic Devices. *Materials*, *18*(12), 2782.

Camiçi, H. C. (2021). *Effects of radiodarkening on the light transmission properties of ytterbium-doped optical fibers* (Master's thesis, Bilkent Universitesi (Turkey)

.
Chapalo, I., Stylianou, A., Mégret, P., & Theodosiou, A. (2024, March). Advances in optical fiber speckle sensing: a comprehensive review. In *Photonics* (Vol. 11, No. 4, p. 299). MDPI.

Chen, S., Wang, C., Xiong, C., Qin, Y., Zhu, J., Shen, Y., & Xiao, L. (2025). Enhancing Single-Mode Characteristics and Reducing Confinement Loss in Liquid-Core Anti-Resonant Fibers via Selective Filling and Geometrical Optimization. *Micromachines*, *16*(4), 438.

Donko, A. L. (2020). *Applications of femtosecond laser micro-machining for fabrication of novel optical sensing devices* (Doctoral dissertation, University of Southampton).

Du, T., Ding, H., Wang, F., Li, Y., & Ma, Y. (2025). Structure-Modulated Long-Period Fiber Gratings: A Review. In *Photonics* (Vol. 12, No. 11).

Efendioglu, H. S. (2017). A review of fiber-optic modal modulated sensors: Specklegram and modal power distribution sensing. *IEEE Sensors Journal*, *17*(7), 2055-2064.

Guo, D., Sun, J., Zhou, X., Yin, S., Li, S., & Qu, Y. (2026). Speckle suppression for UAV tracking using single-photon LiDAR with vibrating MMF and ST-DKDE. *Optics Express*, *34*(4), 6142-6166.

Huang, J., & Ou, Z. (2025). Refractive index engineering: Insights from biological systems for advanced optical design. *Laser & Photonics Reviews*, *19*(15), e00180.

Jiao, L. H., & Pikus, F. (2025). Silicon Waveguides and Temperature-Dependent Performance.

Kant, K., Beeram, R., Cao, Y., Dos Santos, P. S., González-Cabaleiro, L., García-Lojo, D., ... & Santos, I. P. (2024). Plasmonic nanoparticle sensors: current progress, challenges and future prospects. *Nanoscale horizons*, *9*(12), 2085-2166.

Kumar A. J. (2006): Study of fiber optic sugar sensor. Pramana *Journal of Physics*, Vol. 67, No. 2

Li, J., Li, H., Choi, D. Y., Kim, J. T., Lee, W. B., & Lee, S. S. (2024). All-dielectric fiber meta-tip for alignment-tolerant bidirectional interconnect between single-mode and multi-mode fibers. *Advanced Optical Materials*, *12*(36), 2401712.

Liu, X. F., Wang, R., Wang, G. D., Yao, T. F., Miao, H., & Sun, R. (2022). Facile fabrication and optical properties of polymer waveguides with smooth surface for board-level optical interconnects. *Journal of Materials Science: Materials in Electronics*, *33*(34), 26025-26039.

Meehan, B. (2024). *A Comprehensive Materials Approach to Thermal Management in Fiber Lasers* (Doctoral dissertation, Clemson University).

Minds, C., and Light, A. (2016). Technical summaries. *BiOS*, *13*, 18.

Nedoma, J., Krizan, D., Stipal, J., Pereira, L., Bekmurzayeva, A., Tosi, D., ... & Marques, C. (2026). Decade of advancements in light–matter interaction-based optical fiber biosensing: innovations, challenges, and future directions. *Advanced Photonics*, *8*(1), 014004-014004.

Ramachandran, A. V. (2025). Characterization of Composite Fibers.

Shere, W. (2023). *Multi-mode hollow-core anti-resonant optical fibres* (Doctoral dissertation, University of Southampton).

Sun, S., Wu, L., Geng, Z., Shum, P. P., Ma, X., & Wang, J. (2023). Refractometric imaging and biodetection empowered by nanophotonics. *Laser & Photonics Reviews*, *17*(6), 2200814.

Tan, A. J. Y., Ng, S. M., Stoddart, P. R., & Chua, H. S. (2020). Theoretical model and design considerations of U-shaped fiber optic sensors: A review. *IEEE Sensors Journal*, *20*(24), 14578-14589.

Tuomola, P. (2023). Beam Shaping in optical multi-mode fibers.

Wang, X. (2023). Multimode optical waveguide shape sensing based on speckle gram Classification.

Xin, X. (2026). *Advanced Optical Fiber Transmission Systems*. Springer Nature.

Yang, D., Shen, H., Han, H., & Liu, J. (2025). Numerical Investigation of Temperature-Induced Attenuation in Fibers for High-Temperature Well Applications.

Zhao, W., Wu, H., Fu, Y., Ge, J., Yang, H., & Zhang, S. (2023). Design of a transportable miniaturized optical reference cavity with flexibly tunable thermal expansion properties. *Frontiers in Physics*, *10*, 1080196.